NJC

Accepted Manuscript

This article can be cited before page numbers have been issued, to do this please use: D. Zhang, N. Li, Y. Ma, R. Wang, J. Wang and J. Wang, *New J. Chem.*, 2018, DOI: 10.1039/C8NJ00589C.

ROYAL SOCIETY OF CHEMISTRY

rsc.li/njc

View Article Online
DOI: 10.1039/C8NJ00589C

NJC

PAPER

New strategy for the azido-ascorbic acid reaction: a convenient chemosensor and its imaging in garlic slice tissues

Received 00th January 2018,
Accepted 00th January 2018

DOI: 10.1039/x0xx00000x

www.rsc.org/

Dan Zhang, Na Li, Yiming Ma, Ruixue Wang, Jinyi Wang, Junru Wang*[a]

Ascorbic acid (AA) is a vital nutritional factor in many fruits and plants, and abnormal levels of AA are closely associated with several diseases. Therefore, the development of convenient methods for monitoring AA levels in biological systems is of great importance. In this work, we designed and synthesized three chemosensors for the rapid turn-on detection of AA via a new strategy for the azido-ascorbic acid reaction. The chemosensors were based on a 1,8-naphthalimide moiety with the azide group at different sites (probes 1, 2, and 3). The experimental results demonstrated that probe 2 showed high selectivity toward AA, having an experimental limit of detection of 74 nM. Its reduction was easier than that of probe 3 with a 3-substituted azide group. Moreover, probe 2 was successfully used for imaging of AA in garlic slice tissue for the first time.

Introduction

As one of the most important vitamins, ascorbic acid (AA) exists in many fruits and plants, including fresh jujubes, lemons, kiwis, and garlics. AA has multiple functions in vivo, not only maintaining the body's normal physiological function but also participating in various reactions in the body.[1] In particular, AA effectively functions in vivo as an enzyme cofactor, antioxidant, and nutritional factor. As a cofactor, AA is necessary in collagen synthesis and the hydroxylation of lysines and prolines on collagen propeptides by prolyl hydroxylases.[2] AA, as an active antioxidant, can prevent cell damage in free-radical-induced diseases.[3] Unfortunately, AA cannot be synthesized in the human body, and must be obtained from the ingestion of food to maintain the necessary content for the human body.[4] As is well known, lack of AA leads to scurvy. Conversely, excessive intake of AA also results in diarrhea and the formation of urinary stones.[5] Thus, monitoring and imaging AA in garlic, which is a common food with diverse medical uses, are of great significance in disease diagnosis.

Several analytical methods have been used to detect AA in samples, such as chemiluminescence, high-performance liquid chromatography (HPLC), electrochemistry, and ultraviolet (UV)–visible spectrophotometry. Among these measurement techniques, chemiluminescence methods[6] are mainly used for heavy-metal-containing samples. HPLC analysis[7] is limited by complicated sample preparation, expensive reagents, and a large number of operational steps. Electrochemical methods are limited by the complex preparation of electrodes and low selectivity. Relative to fluorescence analysis,[8, 9] the drawbacks of UV–visible spectrophotometric methods[10] include limited linear range and relatively low sensitivity. However, in recent years, fluorescent chemosensors with high sensitivity have been used for the quantitative detection of AA based on redox reactions[11-15] in samples, due to the advantages of high selectivity, rapid response and easy operation. For example, various nanomaterials possessing good membrane permeability and excellent biocompatibility have been used to detect AA. These nanomaterials include quantum dots,[11, 16] MnO_2 nanosheets,[17] carbon nanomaterials,[18, 19] and silica nanoparticles. Additional quenching compounds, such as MnO_2,[4, 16, 20] cobalt oxyhydroxide,[21, 22] Cr(VI),[23-25] $KMnO_4$,[26] Ce^{4+},[27] Fe^{3+},[28] and Cu^{2+},[3, 29-31] are combined with the nanomaterials to quench the fluorescence on the basis of the inner filter effect (IFE). One commonplace disadvantage of this approach is that the systems used for these nanomaterial sensors are not environment-friendly and are extremely complex. Nevertheless, fluorophores linked to nitroxide radicals are typically prepared to detect AA without any quencher, because the nitroxide radical spins efficiently result in florescence quenching.[2, 32-35] In addition, Kong *et al.*[36] reported fluorescent probes based on facile carbon dots for the ultrasensitive detection of AA via a non-

[a] Shaanxi Key Laboratory of Natural Products & Chemical Biology, College of Chemistry & Pharmacy, Northwest A&F University, Yangling, Shaanxi, P.R. China, 712100, E-mail: wangjunru@nwsuaf.edu.cn

View Article Online
DOI: 10.1039/C8NJ00589C
ARTICLE Journal Name

oxidation reduction strategy. However, these methods had relatively high detection limit and long reactive time towards AA. We discovered that azido-substituted fluorescent dyes without the addition of other quenching agents could be employed to detect AA rapidly. A distinct comparison between this work and the literature was undertaken (see Table S1), and indicated that **probe 2** obtained using a simple synthetic method was first used for the direct detection of AA in garlic tissues via a new strategy of azido-ascorbic acid reaction with a short response time.

Due to strong fluorescence and good photostability of 1,8-naphthalimide derivatives, a 1,8-naphthalimide moiety with a 4-substituted azide group acting as the fluorophore has been used to develop H_2S with a very long response time in previous work.[37-40] The main mechanism is the reduction of 4-substituted azido derivatives by H_2S, affording the amino products, usually resulting in absorption redshift and emission enhancement via the intramolecular charge transfer process.[40] Surprisingly, the 1,8-naphthalimide moiety with a 4-substituted azide group was found to be reduced by AA in 1 min. The product of the reaction of the 4-substituted azide group with AA was also the amino product. We thus speculated whether a 1,8-naphthalimide moiety with a 3-substituted azide group could be reduced by AA. Thus, three probes based on the 1,8-naphthalimide moiety with an azide group at different sites (Scheme 1 and Fig. S1) were designed and synthesized for the highly selective detection of AA. The following advantages were considered: (1) according to previous studies on the time-consuming reaction, 4-amino-1,8-naphthalimide can be quickly obtained using the new reactive strategy; (2) the oxidizability of the azide group at different sites can be evaluated; (3) **probe 2** could be used to recognize and visualize AA in garlic slice tissue through the blue and green emission channels.

Experimental

Materials and reagents

All solvents and chemicals were purchased from commercial suppliers and were used without further purification. Water used was ultrafilter deionized.

Apparatus

Column chromatography was performed on silica gel (200–300 mesh). Thin-layer chromatography (TLC) was carried out on silica gel plates (60 F-254) using UV light to monitor the reaction. NMR spectra were obtained using a Bruker 500 Avance III spectrometer. Mass spectrometry (MS) data were obtained with high-resolution ion mobility LC–MS instruments (AB Sciex TripleTOF 5600). Absorption and emission spectra were obtained using a Shimadzu 1750 UV–visible spectrometer and an RF-5301 fluorescence spectrometer (Japan), respectively. HPLC was carried out using Shimadzu LC-15C instruments. Fluorescent images of garlic slice tissues were obtained by fluorescence microscopy (Leica DM6 B).

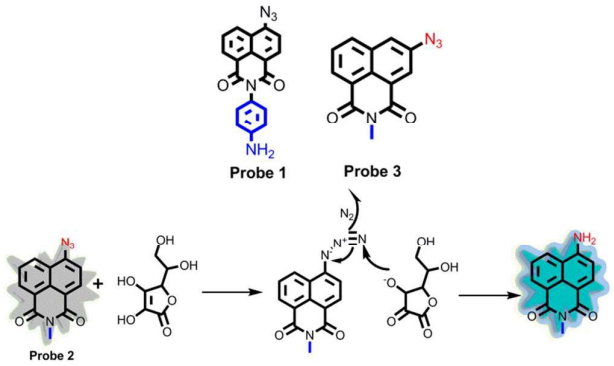

Scheme 1. The structure of the probes.

Synthesis of intermediates and probes

Synthesis of probe 1. A solution of compound **1** (500 mg, 1.8 mmol) and NaN_3 (234 mg, 3.6 mmol) in 20 mL of dimethylformamide (DMF) was stirred for 15 h at room temperature. After 60 mL of cold water was added to the mixed system, a yellow precipitate was collected by filtration and washed three times with water. The yellow solid residue was used directly for the next reaction. To a suspension of compound **2** (239 mg, 1 mmol) in 70 mL of ethyl alcohol was added *p*-phenylenediamine (324 mg, 3 mmol), which was heated to reflux overnight. After cooling to room temperature, the mixture was concentrated and then purified by column chromatography (petroleum ether/CH_2Cl_2 = 1:3, v/v), to give **probe 1** (178 mg) in 54% yield (Fig. 1).

^{1}H NMR (500 MHz, $CDCl_3$) δ 8.64 (dd, *J* = 7.4 Hz, 2H), 8.48 (d, *J* = 8.2 Hz, 1H), 7.77 (t, *J* = 7.5 Hz, 1H), 7.49 (d, *J* = 7.8 Hz, 1H), 7.07 (d, *J* = 7.9 Hz, 2H), 6.81 (d, *J* = 8.0 Hz, 2H), 3.83 (s, 2H); ^{13}C NMR (125 MHz, $CDCl_3$) δ 164.53, 164.07, 146.70, 143.59, 132.58, 132.06, 129.54, 129.25, 128.92, 126.90, 125.73, 124.53, 122.93, 119.25, 115.70, 114.75; MS (ESI) $[M+H]^+$ 330.32 (calculated), 330.33 (found) (Figs. S13-S15).

Synthesis of probe 2. To an ethyl alcohol solution of compound **2** (239 mg, 1 mmol) was added methylamine (62 mg, 2 mmol). The reaction mixture was stirred and heated to reflux for 8 h. After cooling to room temperature, the mixture was concentrated and then purified by column chromatography (petroleum ether/CH_2Cl_2 = 1:1, v/v), to obtain **probe 2** (189 mg) in 75% yield (Fig. 2).

^{1}H NMR (500 MHz, $CDCl_3$) δ 8.61 (d, *J* = 6.4 Hz, 1H),

DOI: 10.1039/C8NJ00589C

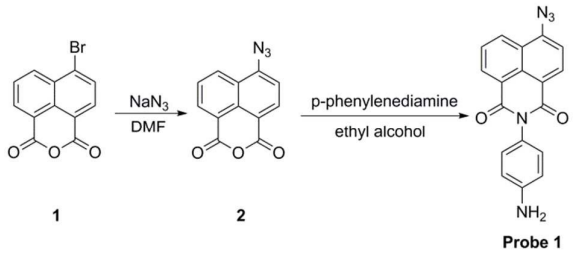

Fig. 1 The synthetic route for **probe 1**.

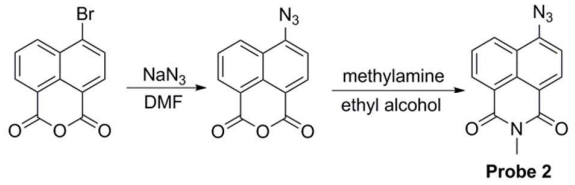

Fig. 2 The synthetic route for **probe 2**.

8.57 (d, *J* = 7.9 Hz, 1H), 8.49 (d, *J* = 7.8 Hz 1H), 7.88-7.62 (m, 1H), 7.45 (d, *J* = 7.9 Hz, 1H), 3.55 (s, *J* = 8.6 Hz, 3H). ^{13}C NMR (125 MHz, $CDCl_3$) δ 164.07, 163.85, 143.31, 132.23, 131.64, 129.06, 128.83, 126.78, 124.36, 122.54, 118.70, 114.70, 27.05. MS (ESI) $[M + Na]^+$ 275.23 (calculated), 275.27 (found) (Figs. S16-S18).

Synthesis of probe 3. Compound **3** (396 mg, 2 mmol) and methylamine (93 mg, 3 mmol) were mixed in 80 mL of ethyl alcohol, and the mixed solution was heated to about 80°C for 8 h. After cooling to room temperature, the mixture was concentrated and then purified by column chromatography (petroleum ether/CH_2Cl_2 = 1:1, v/v), to obtain compound **4** (342 mg) in 81% yield.

$Al(NO_3)_3{\cdot}9H_2O$ (1.1 g, 3 mmol) was added to a solution of compound **4** (211 mg, 1 mmol) in CH_2Cl_2 (40 mL). Then, a solution of acetic acid (2.5 mL) and acetic anhydride (6.5 mL) was added dropwise with magnetic stirring. The mixture was subsequently heated to 70°C for 24 h. After cooling to room temperature, 30 mL of ultrapure water was added, and the pH changed from 2 to 6. After filtering the aqueous solution, the white precipitate obtained was washed with ultrapure water, to give compound **5**.

Compound **5** (256 mg, 1 mmol) was dissolved in methyl alcohol (70 mL). Hydrazine hydrate (256 μL) and Pd/C (catalyst, 50 mg) were then added, and the mixture stirred at 90°C for 6 h. After filtering off the Pd/C, the cooled mixture was evaporated under reduced pressure. The crude product was separated by silica gel column chromatography with dichloromethane as the eluent, to obtain compound **6** (131 mg) with a yield of 58%.

Pure compound **6** (226 mg, 1 mmol) was dissolved in 3 mL of DMF in an ice-salt bath. Then, 1 mL of 30% HCl was added dropwise to the solution. After 3 min, $NaNO_2$ (207 mg, 3 mmol) dissolved in 5 mL of distilled water was added dropwise at 0°C. After 40 min, NaN_3 (195 mg, 3

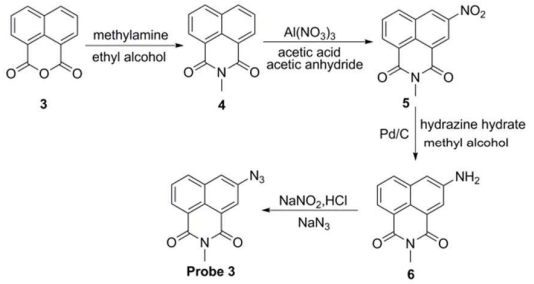

Fig. 3 The synthetic route for **probe 3**.

mmol) dissolved in 5 mL of distilled water was added to the mixture. The solution was then stirred at room temperature overnight. Next, the pH was changed from 2 to 8, and the precipitate obtained was filtered and washed with distilled water. The obtained crude product was separated by silica gel column chromatography, to give **probe 3** (168 mg, 67%) (Fig. 3).

^{1}H NMR (500 MHz, $CDCl_3$) δ 8.56 (dd, *J* = 7.3, 1.0 Hz, 1H), 8.29 (t, *J* = 9.9 Hz, 1H), 8.15 (dd, *J* = 8.2, 0.6 Hz, 1H), 7.82–7.78 (m, 2H), 3.60 (s, 3H). ^{13}C NMR (125 MHz, $CDCl_3$) δ 164.09, 163.62, 139.55, 132.80, 132.64, 130.39, 128.04, 125.53, 124.54, 123.21, 122.73, 121.28, 27.17. MS (ESI) $[M + Na]^+$ 275.06 (calculated), 275.05 (found) (Figs. S19-S21).

Sample preparation and titration

The probe stock solutions were prepared in CH_3CN. Phosphate-buffered saline (PBS) buffers were prepared using ultrapure water. Stock solutions of amino acids and sodium sulfide were dissolved in ultrapure water. Stock solutions of probes (1.0×10^{-3} M) were prepared in CH_3CN and then further diluted to 1.0×10^{-5} M for the experiments. UV and fluorescence spectra were monitored within 30 s.

Calculation of the fluorescence quantum yield

$$\Phi_{\text{unk}} = \Phi_{\text{std}} \times \left(\frac{I_{unk}}{I_{std}}\right) \times \left(\frac{A_{std}}{A_{unk}}\right) \times \left(\frac{n_{unk}}{n_{std}}\right)^2$$

The fluorescence quantum yield of the sample was calculated using quinine sulfate as the standard (Φ = 0.54, 0.1 M H_2SO_4). In this equation, Φ_{unk} and Φ_{std} are the fluorescence quantum yields of the sample and the standard, respectively; I_{unk} and I_{std} are the integral areas of the fluorescent spectra, respectively; A_{unk} and A_{std} are the absorbances of the sample and the standard at the excitation wavelength, respectively; and n_{unk} and n_{std} are the refractive indexes of the corresponding solution, respectively.

Results and discussion

View Article Online
DOI: 10.1039/C8NJ00589C

Fluorescence spectra on detection of AA

All three chemosensors (**probes 1**, **2**, and **3**) were investigated to evaluate the fluorescent detection of AA in 10 mM of PBS buffer (pH 7.4, containing 10% CH_3CN) (Fig. 4). Prior to reaction with AA, **probe 1** was weakly fluorescent, due to the presence of the quenching group (azido). On addition of AA, **probe 1** showed no fluorescence enhancement resulting from the photoinduced electron transfer (PET) process.[41] Under the same conditions, **probe 2** (10 μM) exhibited a maximum absorption at 360 nm and displayed very weak fluorescence. On addition of 2 equiv of AA, the absorption intensity at 460 nm increased, while the intensity at 360 nm decreased (Fig. 5A). The results indicated that **probe 2** was capable of reacting with AA. In accordance with the absorption spectrum, 360 nm was selected as the main excitation wavelength. For **probe 2**, the addition of AA resulted in a marked and rapid increase in fluorescent intensity at 480 nm, with a good linear relationship (Figs. 5B and S1). At the same time, the solution started to show a bright blue fluorescence that was highly visible to the naked eye (observed under a portable 365 nm UV lamp) (Fig. 5B). An approximate 20-fold turn-on was observed after 30 s, with the fluorescence quantum yield increasing from 0.0039 to 0.05, with quinine sulfate as the reference (Fig. S2). The fluorescence quantum yields of **probes 1** and **3** were 0.00045 and 0.0057, respectively. The detection limits of **probe 2** for recognizing AA reached 7.4×10^{-8} M (3s/slope), indicating that **probe 2** was highly sensitive to AA. However, **probe 3** with a 3-substituted azide group showed no response toward AA, and the absorption spectra of **probe 3** on addition of AA showed no change, which illustrated that AA was incapable of reacting with **probe 3** (Figs. 4 and S3). For **probe 2**, the fluorescent intensity could be controlled through the 4-substituented azide group[38-39], while the structure of **probe 3** with the 3-substituented azide group was relative inert[42]. We also explored the effect on the reactive activity of 4-substituented azide group of **probe 1** through modification of other site. Thus, **probe 2** was identified as the key chemosensor for further study.

Selectivity of probe 2 with different ions and biological molecules

The selectivity of **probe 2** was further investigated in the presence of common cations, reactive oxygen species, and biothiols. Under the same conditions, the addition of 2 equiv of biologically relevant species (SO_4^{2-}, K^+, Mg^{2+}, NH_4^+, CO_3^{2-}, Ca^{2+}, Fe^{2+}, NO_2^-, Na^+, hydroquinone (HQ), glucose, dopamine (DA), bovine serum albumin (BSA), H_2O_2, ATP, NaClO, uric acid (UA), His, Ser, Trp, glutathione (GSH), Cys, Hcy, and Na_2S induced no marked turn-on fluorescence responses (Fig. 6). An equal amount of Na_2SO_3 reductant caused no change in the fluorescence spectra of **probe 2** (Fig. S4). In previous reports,[32–35] 1,8-naphthalimide moieties with a 4-substituted azide group were used to detect H_2S, affording the amino products in 60 min, while **probe 2** with a 4-substituted azide group was found to be reduced by AA in 1 min in this paper.

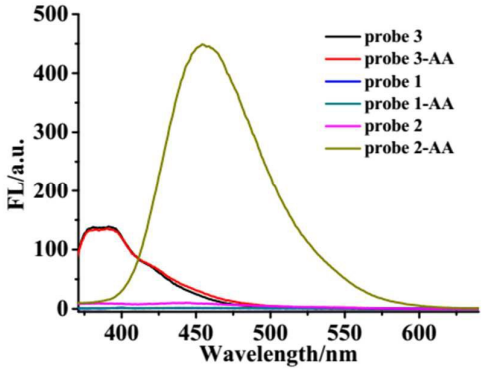

Fig. 4 Fluorescence spectra of **probes 1**, **2**, and **3** (10 μM) on addition of AA (2 equiv). λ_{ex} = 360 and 350 nm, and the slit was 3. Data was collected 30 s after the addition of AA. All the solutions were in PBS/CH_3CN buffer (9:1, v/v, pH 7.4).

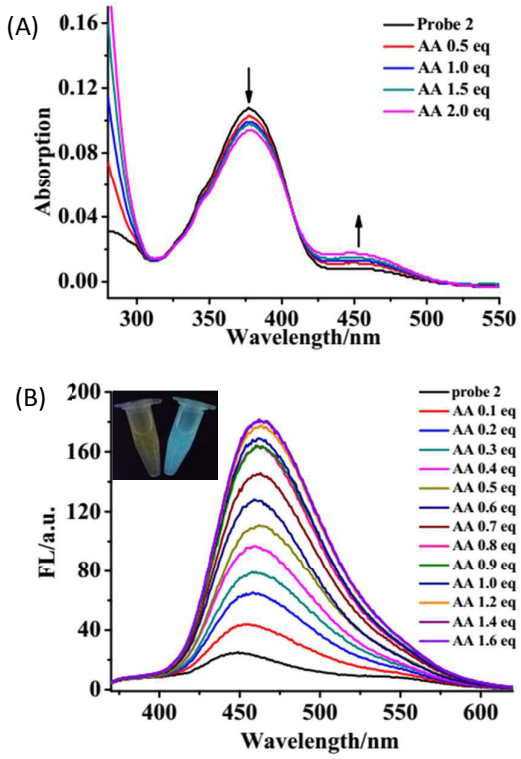

Fig. 5 (A) The absorption spectral change of **probe 2** (10 μM) on addition of 2 equiv of AA. (B) The fluorescence spectral change of **probe 2** (10 μM) on addition of AA, λ_{ex} = 360 nm. All the solutions were in PBS/CH_3CN buffer (9:1, v/v, pH 7.4). Inset: photograph of **probe 2** in the absence and presence of 2 equiv of AA, excited by a hand-held UV lamp (365 nm).

View Article Online
DOI: 10.1039/C8NJ00589C
Journal Name ARTICLE

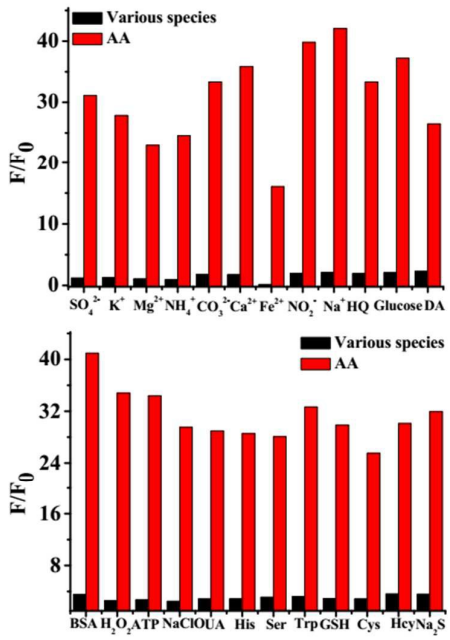

Fig. 6 Fluorescence responses of **probe 2** (10 μM) toward various species: SO_4^{2-}, K^+, Mg^{2+}, NH_4^+, CO_3^{2-}, Ca^{2+}, Fe^{2+}, NO_2^-, Na^+, HQ, Glucose, DA, BSA, H_2O_2, ATP, NaClO, UA, His, Ser, Trp, GSH, Cys, Hcy, and Na_2S. The experiment was performed in PBS/CH_3CN buffer (9:1, pH 7.4), λ_{ex} = 360 nm.

These results indicate that **probe 2** had a high selectivity for the fluorescence detection of AA over other biological species. The stability of three chemosensors (**probes 1**, **2**, **3**) was studied through thermogravimetric analysis. From the figure to know (Fig. S5), the weight loss of **probes 1**, **2**, **3** was only 0.9%, 2.5% and 0.7%, respectively. The results show that these three probes were relatively stable at the temperature range of 25-100°C. Further, the fluorescence intensities of **probe 2** in the absence and presence of AA were pH independent in the range 6-8, demonstrating that **probe 2** could detect AA in the biological environment (Fig. S6).

Sensing mechanism

Probe 2 showed a remarkable and selective fluorescence turn-on response to AA over sulfide when the excitation wavelength was 360 nm. Particular attention was paid to achieving an understanding of the differences in response for **probe 2** when the excitation wavelength was 460 nm. As shown in Fig. 7, an approximate four fold fluorescence enhancement at 540 nm was observed when 2 equiv of AA were added, while the ratio of the fluorescence intensity at 540 nm exhibited only a threefold increase in 15 min when 2 equiv of Na_2S were added. Although H_2S can reduce the azide group of the probes, it was time-consuming for 30-60 min[43]. In this work, the detection process of AA was finished in 1 min. However, Na_2S had no interference in the detection of AA in the same situation due to no chemical reaction between **probe 2** and Na_2S in 1 min. Because of this, we were interested in the mechanism, and investigated the products from the reaction between **probe 2** and AA. First, HPLC showed the appearance of new peaks after the addition of differing equivalents of AA to **probe 2** (0.2 mM) (Fig. S7), which indicated that **probe 2** has been reduced by AA to form a new product. We then investigated whether **probe 1** with a 4-substituted azide group was reduced by AA. As shown in Fig. S8, a peak emerged with a retention time of 6.5 min after the addition of differing equivalents of AA. The product, which was verified through high-resolution MS, was the corresponding 4-substituted amino of **probe 1** (Fig. S22). Although reduced by AA, **probe 1** showed no fluorescence due to the PET process. Therefore, it was hypothesized that the products obtained from the reactions of **probe 2**-AA and **probe 2**-Na_2S were the

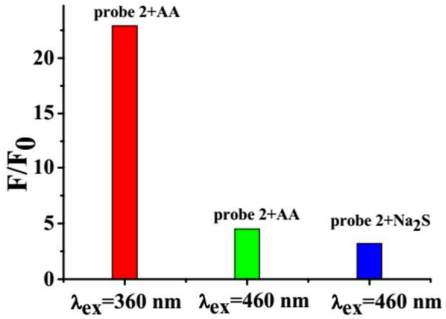

Fig. 7 Fluorescence responses of **probe 2** (10 μM) toward 2 equiv of AA and Na_2S with different excitation wavelengths. The experiment was performed in PBS/CH_3CN buffer (9:1, pH 7.4).

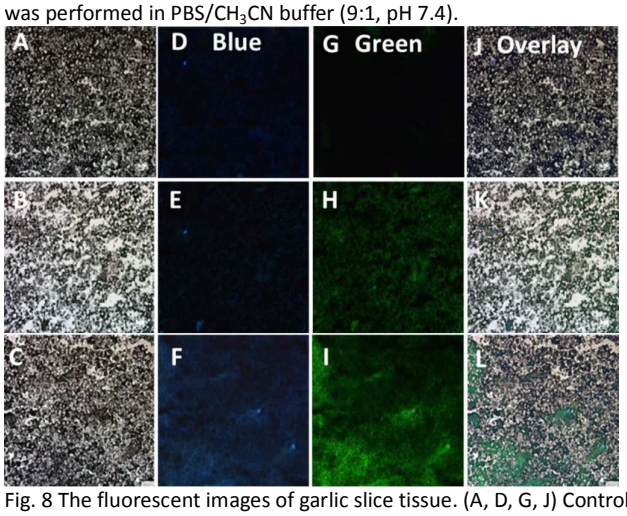

Fig. 8 The fluorescent images of garlic slice tissue. (A, D, G, J) Control experiment. (B, E, H, K) Fluorescent images of garlic slice tissue treated with **probe 2** (40 μM) for 5 min. (C, F, I, L) Fluorescent images of garlic slice tissue pretreated with **probe 2** (40 μM) for 5 min before incubation with AA (40 μM) for 5 min. (D-F) Fluorescence images of AA in garlic slice tissue: emission was at 415–480 nm for the blue channel (excited at 405 nm). (G-I) Fluorescence images of AA in garlic slice tissue: emission was at 495–580 nm for the green channel (excited at 458 nm). Scale bar: 500 μm.

View Article Online
DOI: 10.1039/C8NJ00589C

corresponding 1,8-naphthalimide moieties with a 4-substituted amino. The proposed structure of the products was verified via ^{1}H NMR, ^{13}C NMR, and MS (Figs. S9-S11) (scheme 1). Using this new strategy, we rapidly obtained the 4-amino-1,8-naphthalimide, which was generated from **probe 2**-AA. Moreover, probably because of the solvent effect, this 4-amino-1,8-naphthalimide emitted blue and yellow-green fluorescence in different solvents when illuminated by a hand-held UV lamp (365 nm) (Fig. S12).

Imaging in garlic slice tissues

To further investigate the biological applications of **probe 2**, fluorescence microscopy experiments were performed on garlic slice tissue, which is abundant in AA (79 mg/100 g). First, dehydrated garlic was sliced using a freezing microtome. Unbroken slices were used for fluorescence imaging. Figure 8A shows the blank sample. In the control experiment, the garlic slice was treated with **probe 2** (40 μM) for 5 min, then additional **probe 2** was washed three times with ethyl alcohol (Fig. 8B). The fluorescent microscopy image of the slice showed a little weak blue and green fluorescence at the excitation wavelengths of 405 and 488 nm (Figs. 8E and 8H), respectively, indicating that **probe 2** was capable of reacting with endogenous AA with high sensitivity. In a further experiment, garlic slice tissue was pretreated with **probe 2**, and then incubated with AA (40 μM): significant fluorescence was observed (Figs. 8F and 8I). These results indicate that **probe 2** can be used as a fluorescent label for the specific detection of AA, producing discernible fluorescence responses in garlic slice tissues.

Conclusion

In summary, we designed and synthesized three chemosensors based on a 1,8-naphthalimide moiety with an azide group at different sites for fluorescence turn-on detection of AA via a novel and convenient redox strategy. The results of the investigation showed that the 4-amino-1,8-naphthalimide formed rapidly through the reaction between **probe 2** and AA. Although reduced by AA, **probe 1** with the 4-substituted azide group showed no fluorescence enhancement because of the PET process. In contrast to **probe 3** with a 3-substituted azide group, **probe 2** showed high selectivity toward AA, and was easier to reduce. Moreover, **probe 2** acted as a fluorescent sensor to visualize AA in garlic slice tissues through the blue and green emission channels.

Acknowledgments

We are grateful for financial support from the Open Foundation of the Key Laboratory of Synthetic, Natural Functional Molecule Chemistry of the Ministry of Education (31270388), and from the National Natural Science Foundation of China (81773603).

References

1. L. L. Feng, Y. X. Wu, D. L. Zhang, X. X. Hu, J. Zhang, P. Wang, Z. L. Song, X. B. Zhang and W. Tan, *Anal. Chem.*, 2017, **89**, 4077-4084.
2. Y. Matsuoka, M. Yamato, T. Yamasaki, F. Mito and K. Yamada, *Free Radic. Biol. Med.*, 2012, **53**, 2112-2118.
3. J.-J. Liu, Z.-T. Chen, D.-S. Tang, Y.-B. Wang, L.-T. Kang and J.-N. Yao, *Sens. Actuators B*, 2015, **212**, 214-219.
4. J. Liu, Y. Chen, W. Wang, J. Feng, M. Liang, S. Ma and X. Chen, *J. Agric. Food Chem.*, 2016, **64**, 371-380.
5. G. Hu, Y. Guo, Q. Xue, S. Shao, *Electrochim. Acta*, 2010, **55**, 2799-2804.
6. X. Zhang, L.-X. Ma and Y.-C. Zhang, *Electrochim. Acta*, 2015, **177**, 118-127.
7. A. Khan, M. I. Khan, Z. Iqbal, Y. Shah, L. Ahmad, S. Nazir, D. G. Watson, J. A. Khan, F. Nasir, A. Khan and Ismail, *Talanta*, 2011, **84**, 789-801.
8. Y.-J. Chen and X.-P. Yan, *Small*, 2009, **5**, 2012-2018.
9. H. Chen, R. Li, L. Lin, G. Guo and J. M. Lin, *Talanta*, 2010, **81**, 1688-1696.
10. A. M. El-Zohry and E. Y. Hashem, *Journal of Spectroscopy*, 2013, **2013**, 1-7.
11. P. Zhao, K. He, Y. Han, Z. Zhang, M. Yu, H. Wang, Y. Huang, Z. Nie and S. Yao, *Anal. Chem.*, 2015, **87**, 9998-10005.
12. H. Huang, B. Wang, M. Chen, M. Liu, Y. Leng, X. Liu, Y. Li and Z. Liu, *Sens. Actuators B*, 2016, **235**, 356-361.
13. X. Chen, Y. Xu, H. Li and B. Liu, *Sens. Actuators B*, 2017, **246**, 344-351.
14. N. Li, Y. Li, Y. Han, W. Pan, T. Zhang and B. Tang, *Anal. Chem.*, 2014, **86**, 3924-3930.
15. X. Pan, X. Wang, L. Wang, K. Xu, F. Kong and B. Tang, *Anal. Chem.*, 2015, **87**, 7092-7097.
16. X. Gong, Y. Liu, Z. Yang, S. Shuang, Z. Zhang and C. Dong, *Analytica chimica acta*, 2017, **968**, 85-96.
17. W. Zhai, C. Wang, P. Yu, Y. Wang and L. Mao, *Anal. Chem.*, 2014, **86**, 12206-12213.
18. L. Li, C. Wang, K. Liu, Y. Wang, K. Liu and Y. Lin, *Anal. Chem.*, 2015, **87**, 3404-3411.
19. L. Zhang, F. Liu, X. Sun, G. F. Wei, Y. Tian, Z. P. Liu, R. Huang, Y. Yu and H. Peng, *Anal. Chem.*, 2017, **89**, 1831-1837.
20. G. Li, N. Lv, J. Zhang and J. Ni, *RSC Adv.*, 2017, **7**, 16423-16427.
21. H. M. Meng, X. B. Zhang, C. Yang, H. Kuai, G. J. Mao, L. Gong, W. Zhang, S. Feng and J. Chang, *Anal. Chem.*, 2016, **88**, 6057-6063.
22. Q. Han, Z. Dong, X. Tang, L. Wang, Z. Ju and W. Liu, *J. Mater. Chem. B*, 2017, **5**, 167-172.
23. M. Zheng, Z. Xie, D. Qu, D. Li, P. Du, X. Jing and Z. Sun, *ACS applied materials & interfaces*, 2013, **5**, 13242-13247.
24. H. Rao, Y. Gao, H. Ge, Z. Zhang, X. Liu, Y. Yang, Y. Liu, W. Liu, P. Zou, Y. Wang, X. Wang, H. He and X. Zeng, *Anal. Bioanal. Chem.*, 2017, **409**, 4517-4528.
25. P. Li, Y. Hong, H. Feng and S. F. Y. Li, *J. Mater. Chem. B*, 2017, **5**, 2979-2988.
26. S. Huang, F. Zhu, Q. Xiao, W. Su, J. Sheng, C. Huang and B. Hu, *RSC Adv.*, 2014, **4**, 46751-46761.
27. R. Liu, R. Yang, C. Qu, H. Mao, Y. Hu, J. Li and L. Qu, *Sens. Actuators B*, 2017, **241**, 644-651.

View Article Online
DOI: 10.1039/C8NJ00589C

28. J. Gong, X. Lu and X. An, *RSC Adv.*, 2015, **5**, 8533-8536.
29. G. Xue, Z. Yue, Z. Bing, T. Yiwei, L. Xiuying and L. Jianrong, *J. Lumin.*, 2016, **180**, 146-150.
30. J. Duan, J. Yu, S. Feng and L. Su, *Talanta*, 2016, **153**, 332-339.
31. Y. Zhao, Y. Li, Y. Wang, J. Zheng and R. Yang, *RSC Adv.*, 2014, **4**, 35112.
32. K. Ishii, K. Kubo, T. Sakurada, K. Komori and Y. Sakai, *Chem. Commun.*, 2011, **47**, 4932-4934.
33. T. Yang, B. Zheng, H. Liang, Y. Wan, J. Du and D. Xiao, *Talanta*, 2015, **132**, 191-196.
34. C.-P. Liu, T.-H. Wu, C.-Y. Liu, H.-J. Cheng and S.-Y. Lin, *J. Mater. Chem. B*, 2015, **3**, 191-197.
35. Y. Matsuoka, K. Ohkubo, T. Yamasaki, M. Yamato, H. Ohtabu, T. Shirouzu, S. Fukuzumi and K.-i. Yamada, *RSC Adv.*, 2016, **6**, 60907-60915.
36. W. Kong, D. Wu, G. Li, X. Chen, P. Gong, Z. Sun, G. Chen, L. Xia, J. You and Y. Wu, *Talanta*, 2017, **165**, 677-684.
37. Z. Wu, D. Liang, X. Tang, *Anal. Chem.*, 2016, **88**, 9213-9218.
38. L.A. Montoya, M.D. Pluth, *Chem. Commun.*, 2012, **48**, 4767-4769.
39. L. He, W. Lin, Q. Xu, H. Wei, *Chem. Commun.*, 2015, **51**, 1510-1513.
40. D.-T. Shi, D. Zhou, Y. Zang, J. Li, G.-R. Chen, T.D. James, X.-P. He, H. Tian, *Chem. Commun.*, 2015, **51**, 3653-3655.
41. Y. Wang, A. La, C. Bruckner and Y. Lei, *Chem. Commun.*, 2012, **48**, 9903-9905.
42. T. Liu, F. Huo, J. Li, J. Chao, Y. Zhang and C. Yin, *Sens. Actuators B*, 2016, **237**, 127-132.
43. Z. Wu, D. Liang and X. Tang, *Anal. Chem.*, 2016, **88**, 9213-9218.

View Article Online
DOI: 10.1039/C8NJ00589C

A table of contents entry

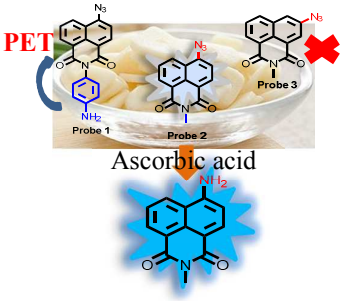

Text: Three chemosensors with azide group at different sites were designed for rapid detection of ascorbic acid in garlic slice tissues.